Table of contents

Solicitation: NNH19ZDA001N-NFDAP

"Juno Observations of Temporal Variability in Jupiter's Magnetosphere"

PI: Marissa Vogt

Scientific/Technical/Management section (15 pages)	2
References	17
Data Management Plan	24
Biographical Sketch for PI Marissa Vogt	26
Biographical Sketch for Co-I Bertalan Zieger	28
Biographical Sketch for Co-I Jeff Morgenthaler	29
Table of Personnel and Work Effort	30
Current and Pending for PI Marissa Vogt	31
Current and Pending for Co-I Bertalan Zieger	32
Current and Pending for Co-I Jeff Morgenthaler	33
Data Archiving in the Planetary Data System (PDS)	34
Budget Narrative and Sub Award Documents	36

Juno Observations of Temporal Variability in Jupiter's Magnetosphere

The objective of the proposed work is to establish the amount of temporal variability observed in Jupiter's middle and outer magnetosphere during Juno's first 16 orbits of Jupiter and determine its likely source(s) and its effects on Jupiter's main auroral emission. We will study how the magnetic field and plasma properties vary on time scales from hours to months. We will compare this variability to two likely drivers of magnetospheric activity: plasma input to the magnetosphere from Io's volcanic activity and predicted changes in the upstream solar wind conditions. We will predict the upstream solar wind conditions using a new propagation model and determine Io's contribution to magnetospheric variability by considering ground-based and Juno radio occultation observations. Our work will represent the first long-term comparison between Earth-based Io plasma torus observations and *in situ* measurements from Jupiter's magnetosphere, which will provide an important first step in understanding radial plasma transport from Io through the magnetosphere. Finally, we will use the observed magnetospheric variability to predict the resulting shifts in Jupiter's main auroral emission, and compare our predictions to Juno UVS and HST auroral images.

1. Introduction

The Juno mission has now completed more than 20 orbits of Jupiter, collecting a wealth of information about Jupiter's magnetosphere and aurora. Juno was preceded by 7 spacecraft flybys and one orbiter (Galileo), which established the basic structure of Jupiter's magnetosphere, illustrated in **Figure 1**. An important feature in Jupiter's magnetosphere is the Io plasma torus (IPT), a ring of plasma trapped on magnetic field lines at Io's orbital radius (5.9 R_J, or Jovian radii). Io, the most volcanically active moon in the solar system, is the primary source of plasma in Jupiter's magnetosphere, filling it with sulfur and oxygen ions at an estimated rate of ~500-1000 kg/s (e.g. Thomas et al., 2004). Another outstanding feature in Jupiter's magnetosphere is an azimuthally directed current sheet which stretches field lines radially in the middle and outer magnetosphere (e.g. Smith et al., 1974); in the inner magnetosphere ($R < 10$ R_J) the field is largely dipolar. As illustrated in **Figure 1**, in the inner and middle magnetosphere ($R <$ ~30 R_J) the current sheet is mostly aligned with the magnetic equator, which is tilted with respect to the jovigraphic equator due to Jupiter's ~10° dipole tilt, and in the outer magnetosphere ($R >$ ~60 R_J) the current sheet is parallel to the solar wind (Behannon et al., 1981).

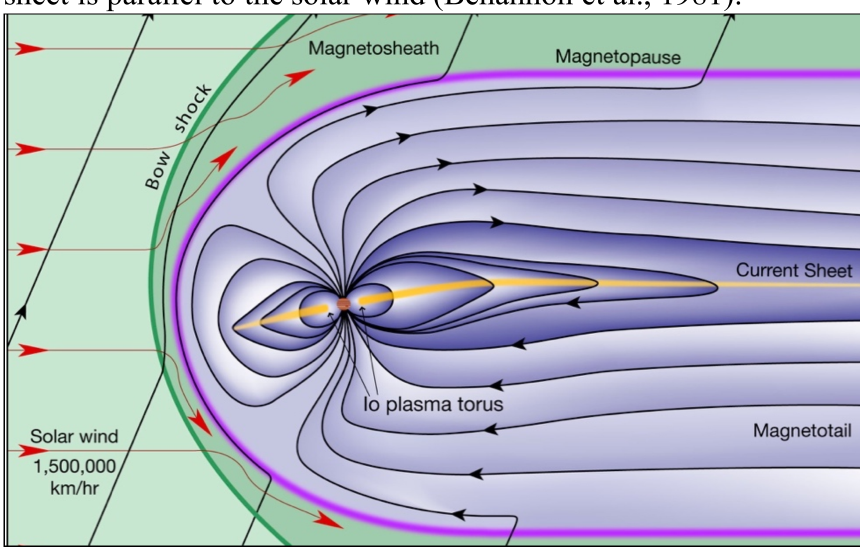

Figure 1. The main features of Jupiter's magnetosphere, shown here in a meridional plane, including the Io plasma torus, current sheet. The magnetic field is mostly dipolar in the inner magnetosphere and highly radially stretched in the middle and outer magnetosphere due to the presence of a strong current sheet. Courtesy Fran Bagenal and Steve Bartlett.

Observations of Jupiter's magnetosphere and aurora show that the system varies on time scales ranging from minutes to years. Several examples of this variability observed in *in situ* datasets from the middle and outer magnetosphere are discussed in more detail in section 3.1, and include magnetic reconnection and plasmoid release; quasi-periodic modulations of the magnetic field, plasma properties, and auroral radio emissions on time scales of ~2-3 days; solar wind compressions or magnetotail loading/unloading events; and changes in the current sheet current density. Changes in Jupiter's aurora, which prior to Juno was primarily imaged using the Hubble Space Telescope (HST), provide a useful diagnostic of temporally-varying physical processes occurring throughout the magnetosphere, since auroral images provide a global view whereas spacecraft measurements are spatially limited.

Jupiter's main auroral emission is associated with a corotation enforcement current (CEC) system in the middle magnetosphere, and is thought to typically map to a radial distance of ~30 R_J (Cowley and Bunce, 2001; Hill, 2001). Variability in the ionospheric position of the main auroral emission, and its brightness, can indicate changes in the CEC system. The CEC system depends on factors like the ionospheric conductivity (e.g. Nichols and Cowley, 2004) and the radial gradient in the magnetospheric plasma azimuthal velocity profile, which in turn depends on the plasma mass loading rate from Io. However, **shifts in the main emission position can also be caused by changes Jupiter's current sheet, which affects in the amount of field line radial stretching** (Grodent et al., 2008), as illustrated in **Figure 2**. As shown in the middle and right panels of Figure 2, increases in the amount of field line stretching lead to an equatorward shift in the ionospheric mapping of a fixed point in the equator. A change in Jupiter's current sheet is the likely explanation for the auroral shifts shown in **Figure 2** because both the main emission *and* the Ganymede footprint (green arrows) shift. (The Ganymede footprint is linked to a fixed 15 R_J in the equator so it is unaffected by changes in the CEC system but is affected by changes in field line morphology.)

In past studies it has been difficult to discern the relative roles of internal and external driving in Jupiter's magnetosphere because the upstream solar wind conditions and Io's

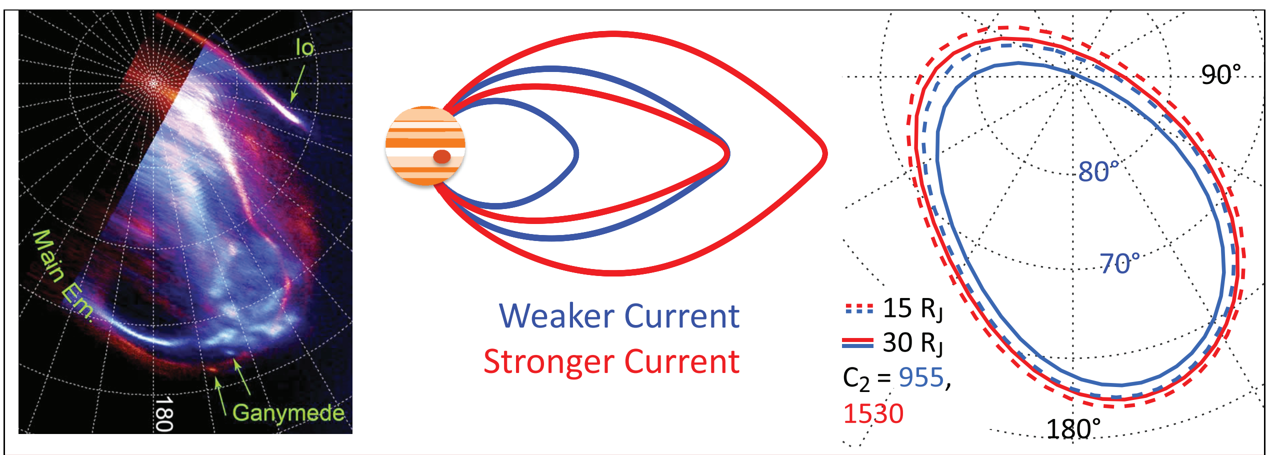

Figure 2. (Left) HST observations of Jupiter's aurora from December 2000 (red) and April 2005 (blue), from Grodent et al. (2008). **(Middle)** Illustration of how changes in the current sheet strength can alter the magnetic field configuration and ionospheric mapping (not to scale). The field lines have been traced from two fixed points in the ionosphere, and the red field lines show a field morphology with a stronger current sheet current density than for the blue field lines. **(Right)** Expected shifts in the ionospheric mapping of 15 R_J and 30 R_J in the equator calculated from variability observed in Jupiter's current sheet by Galileo. Modified from Vogt et al. (2017).

plasma production were observationally unconstrained, though it is likely that both internal and external drivers affect many features of the magnetosphere. For example, theoretical calculations suggest that changes in Jupiter's current sheet could occur as the Jovian magnetic field configuration changes in response to changing solar wind dynamic pressure, P_{Dyn} (e.g. Cowley and Bunce, 2003a, 2003b). However, modeling work has also suggested that internal drivers, like changes in the plasma mass loading rate from Io and magnetospheric density, can also produce significant changes in the Jovian magnetic field configuration (e.g. Nichols, 2011; Nichols et al., 2015). Galileo data have shown changes in Jupiter's magnetic field and auroral radio emissions following the arrival of an interplanetary shock (e.g. Gurnett et al., 2002; Hanlon et al., 2004). However, since upstream solar wind measurements are typically unavailable (the Cassini flyby of Jupiter, while Galileo was located in Jupiter's magnetosphere, is the only exception), the role of the solar wind in Jupiter's magnetosphere has long been an area of debate (McComas and Bagenal, 2007; Cowley et al., 2008). Because Io, and not the solar wind, is the main source of plasma in Jupiter's magnetosphere, it is likely that internal drivers, including variability in Io's plasma production, are the most significant source of temporal variability in Jupiter's magnetosphere.

Unfortunately, the rate of plasma production from Io is difficult to measure. Material released from Io's SO_2 atmosphere forms a neutral cloud near Io's orbit and is later ionized through charge exchange and electron impact ionization, forming a plasma torus (Thomas et al., 2004). Io's neutral production rate is highly variable, ranging from ~0.4 to ~1.3 tons/s on time scales of years (e.g. Delamere and Bagenal, 2003). Not all this gas is ionized. The rate at which plasma is introduced to the magnetosphere is also likely to be highly variable and is difficult to constrain. Many studies of variability in the conditions in and near the Io plasma torus (IPT) have relied on ground-based observations of Io's sodium nebula brightness, which can be used to infer variation in Io's volcanic activity (e.g. Mendillo et al. 2004, Yoneda et al. 2015). Sodium is a minor component of Io's atmosphere and forms a large neutral cloud or nebula that extends for hundreds of R_J and is easily visible from the Earth (e.g. Mendillo et al., 1990). While changes in the sodium nebula brightness do not necessarily indicate a change in Io's plasma production rate, it can be a useful proxy for plasma density because the diffuse nebula component results from ion recombination (Wilson et al., 2002; Brown and Bouchez, 1997; Nozawa et al., 2005). Published timescales for radial plasma transport outward from Io's orbit into the middle magnetosphere vary from 10 days to several months (Delamere and Bagenal, 2003; Tsuchiya et al., 2018).

To date, there have been no long-term comparisons between Earth-based Io plasma torus observations and *in situ* measurements from Jupiter's magnetosphere. Such a comparison would provide crucial information about how the variability in the IPT and in Io's plasma production rate affect magnetospheric activity. The EUV spectrometer on the JAXA Hisaki satellite has monitored Jupiter's aurora and sulfur emissions from the IPT, but its guide camera failed in 2016 so there has been very little overlap with Juno observations from the magnetosphere (Kimura et al., 2017). Galileo-era ground-based observations provided only irregular monitoring (e.g. Thomas et al., 2001) and none were actually tied to *in situ* data for a system-wide perspective.

Ground-based observations of the IPT are now available with concurrent Juno observations from Jupiter's magnetosphere (Morgenthaler et al., 2019, see section 2). **These ground-based observations recorded a large volcanic event on Io during 2018, providing a unique opportunity to establish how such an event affects Jupiter's magnetosphere through analysis of *in situ* Juno data.** We propose to analyze Juno data to establish the amount of temporal variability observed in Jupiter's middle and outer magnetosphere during Juno's first ~2.5 years in orbit. We will determine how the magnetic field, plasma, and auroral radio emissions varied on time scales from hours to months, and relate these changes to variability concurrently observed in Jupiter's UV auroral emissions with Juno and HST. We will also examine the relative roles of the solar wind and Io in driving temporal variability through analysis of the concurrent ground-based IPT observations and predictions of the upstream solar wind using a model that propagates Earth-based solar wind data out to Jupiter's orbit at 5.2 AU. Our work will be an important first step in understanding radial plasma transport from Io through the magnetosphere and in observationally constraining the timescales associated with radial plasma transport. **Our work is motivated by the following questions:**

1) What is the nature and source(s) of temporal variability in Jupiter's magnetosphere?

2) How does temporal variability in Jupiter's magnetosphere influence Jupiter's aurora?

3) How, and on what time scale, does variability in Io's plasma production influence the magnetosphere?

We will build on two previous studies led by PI Vogt. In Vogt et al. (2017) we examined temporal variability in Jupiter's current sheet by fitting Galileo magnetometer data to a current sheet model and calculating how Jupiter's current sheet current density changed from one orbit to another. In Vogt et al. (submitted, sites.bu.edu/marissavogt/files/2019/08/2019JA026950R.pdf, under revision at JGR) we examined statistical links between the predicted solar wind conditions and magnetospheric activity.

However, our previous work was hindered by the lack of long-term monitoring of the IPT for comparison to the Galileo data. For example, in Vogt et al. (2017) we were unable to identify a clear correlation between variability in Jupiter's current sheet and *either* internal or external drivers. Because we required a long-term (1996-2003) measurement, we attempted to use ground-based observations of the infrared brightness of Loki (Rathbun et al., 2002), the largest volcano on Io, as a proxy for Io's plasma production. We concluded that further investigation was needed, including a better proxy for Io plasma production and time lags associated with outward plasma transport. **The work we propose here will directly address this issue by using long-term ground-based *measurements* (not a proxy) of the Io plasma torus.** Additionally, improvements in the solar wind propagation model to be used will enable prediction of all three components of the interplanetary magnetic field (IMF), which is crucial for fully understanding the interaction between the solar wind and Jupiter's magnetosphere.

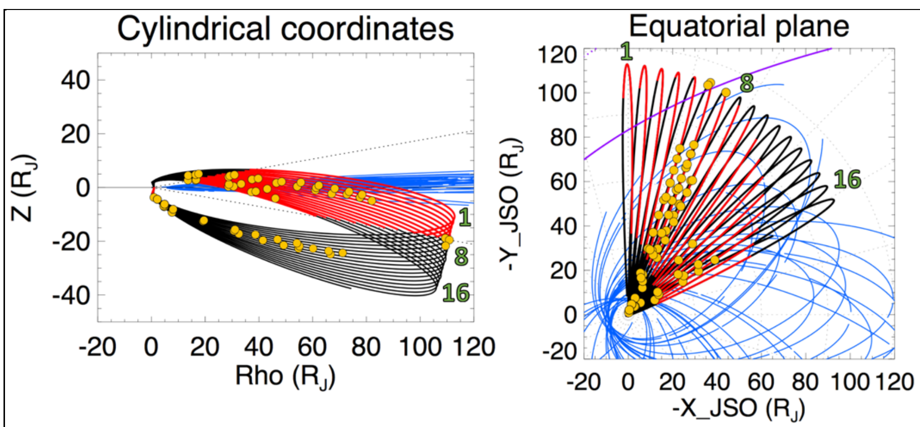

Figure 3. Juno's orbital trajectory (black), with intervals within 10º of the equator shown in red. Galileo's orbit is shown in blue. Green text indicates orbit #s. Orange dots indicate Juno's position at the time of HST images.

2. Data to be used in this study

We will take advantage of a diverse set of data, focusing on Juno *in situ* measurements of the magnetic field and plasma conditions in Jupiter's magnetosphere and remote auroral images, and also taking advantage of concurrent ground-based observations of the conditions in the Io plasma torus and Hubble Space Telescope (HST) images of Jupiter's UV aurora. We will analyze data covering Juno's first 16 orbits, or perijoves (PJs), of Jupiter, corresponding roughly to the time period from Jupiter Orbit Insertion (JOI) in July 2016 through the end of 2018. These Juno data were publicly archived in the PDS at least 30 days before the Step-2 NFDAP deadline.

Juno is in a 53-day polar orbit with an apojove of 113 R_J , perijove passes as close as 0.07 R_J altitude, and inclination up to 105.5º (Bolton et al., 2017). The spacecraft spins at 2 rpm. The left panel of **Figure 3** shows its orbit projected into the equatorial plane. The orbital tilt increases during each orbit so that with each successive orbit, or perijove (PJ), Juno spends less time near the equatorial plane and the equatorial crossing point of its orbit moves radially inward. Juno's orbit has several benefits for studying temporal variability in the magnetosphere. The trajectory does not change much spatially from orbit to orbit, making it likely that any observed differences in successive orbits are due to temporal and not spatial effects. Second, Juno's inclined orbit provides the opportunity to observe both the magnetospheric lobe field and Jupiter's current sheet, which is located roughly at the magnetic equator and passes over the equator every ~5 hours due to Jupiter's 10º dipole tilt. The current sheet is accessible to Juno during the inbound portion of the first ~16 orbits (red lines in **Figure 3**) and is important for identifying reconnection events and measuring the current sheet variability, while the lobe field observations enable easy identification of compressions and tail loading/unloading. We will use data from the following Juno instruments:

- **MAG** (Magnetometer; Connerney et al., 2017) – Vector fluxgate magnetometer measuring the magnetic field components; we will use data with a time resolution of 1 second per vector
- **JEDI** (Juno Energetic particle Detector Instrument; Mauk et al., 2017) – Measures energy and pitch angle distributions for electrons from 40 to 500 keV and energy, pitch angle, and ion composition distributions for ions at ~20-50 keV to more than 1 MeV. Time resolution as high as 0.5 seconds in the auroral region.
- **JADE** (Jovian Auroral Distributions Experiment; McComas et al., 2017) – Provides energy spectra and pitch angle distributions for electrons at 0.1-100 keV and ions 5 eV - 50 keV, also measures ion composition from 1 to 50 amu. Time resolution ranges from 30 seconds to 10 minutes in low rate science mode depending on bandwidth.
- **Waves** (Juno WAVES Investigation; Kurth et al., 2017) – Provides electric spectra at frequencies 50 Hz to 40 MHz and magnetic spectra at frequencies 50 Hz to 20 kHz, with a time resolution of 30 seconds per spectra (in apoapsis mode)
- **UVS** (Ultraviolet Spectrograph; Gladstone et al., 2014) – a photon-counting imaging spectrograph with a spectral range of 68-210 nm. The Juno-UVS slit is oriented perpendicular

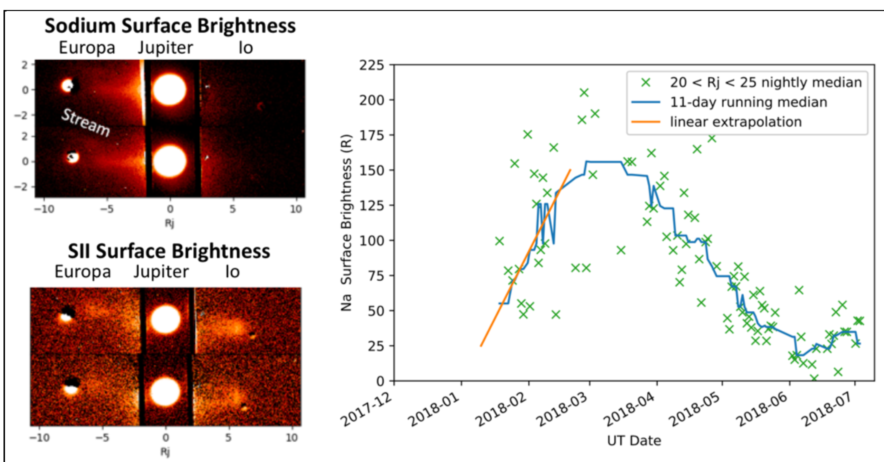

Figure 4. (Left) Inner portion of Na 5890 Å (top) and [SII] 6731 Å (bottom) images recorded contemporaneously by IoIO on 2018-06-06. **(Right)** IoIO sodium nebula observations from 2018 showing a long-term increase. From Morgenthaler et al. (2019), figure 2.

to the spin plane of Juno and as such scans across the sky every spin. Complete maps of Jupiter's auroral regions are produced by stepping the scan mirror between consecutive spins and then stitching scan maps together.

Additionally, we will consider **Juno radio occultation observations of the Io plasma torus** (Phipps and Withers, 2017; Phipps et al., 2018, 2019), which can provide a snapshot view of the IPT density once per Juno orbit. These observations are made using Juno's gravity science instrument (Asmar et al., 2017) and provide a measurement of total electron content (TEC) as a function of time for a few hours near periapsis. The torus plasma density can be calculated from the maximum TEC value observed during that time. IPT radio occultations can be conducted when the high-gain antenna is pointed toward Earth (i.e. when Juno is not making microwave radiometer observations), meaning that IPT densities are available for PJs 1, 3, 6, 8, 10, 11, 13, 14, and 15.

We will monitor the density of the IPT via **ground-based IoIO images of the Io plasma torus**. IoIO is the Io Input/Output facility, a dedicated 35 cm robotic telescope located 100 km east of Tucson, built with the support of a 5-year NSF grant (2018-2023) to Co-I Jeff Morgenthaler. IoIO has provided near-continuous monitoring since its commissioning in March 2017. It measures gas-rich volcanic events via the sodium nebula (Na 5893Å) and S+ torus ([SII] 6731 Å). Example IoIO data, which are recorded on a 6-minute cadence whenever Jupiter is visible, are shown in **Figure 4**. IoIO images of the IPT provide important diagnostics of radial diffusion from the mass source region in two ways: (1) The total brightness of the IPT tracks the amount of mass at the source region and (2) the dawn-dusk displacement of the IPT tracks material moving toward the magnetotail (Barbosa and Kivelson, 1983; Brown and Bouchez, 1997) and/or compression of the

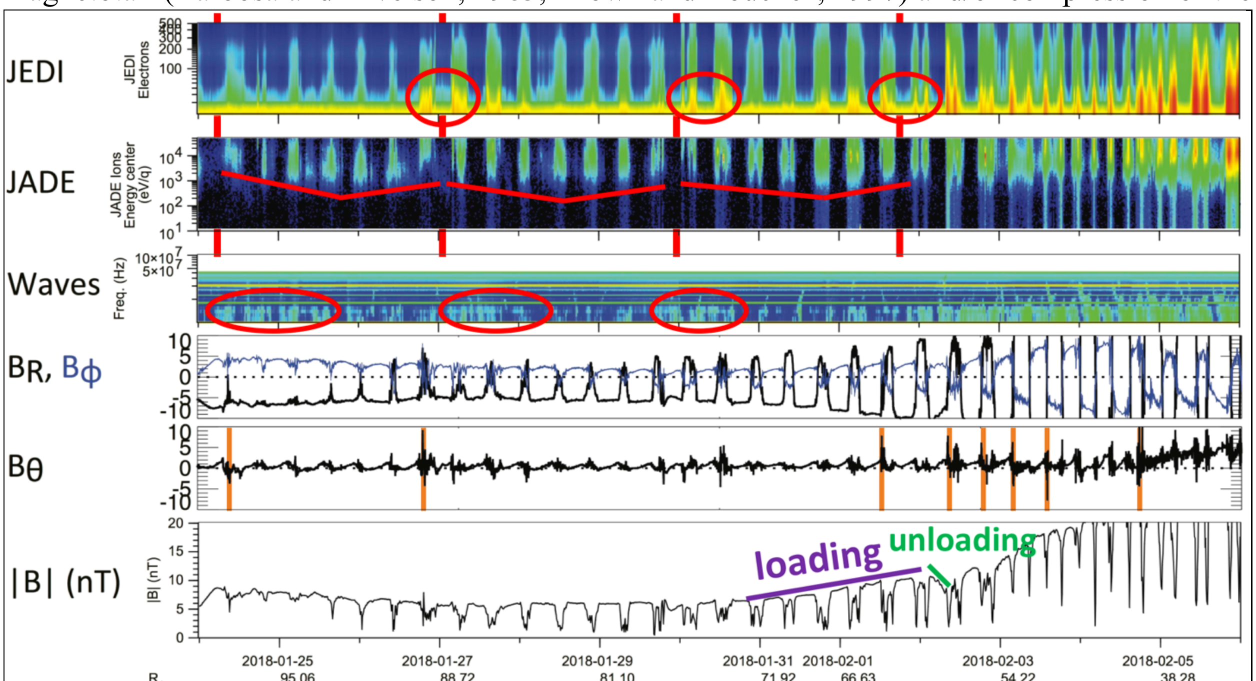

Figure 5. Juno observations from the inbound portion of PJ11, from 24 Jan. through 5 Feb. 2018, showing several examples of temporal variability. From top: JEDI electron energy spectrogram, JADE ion energy spectrogram, Waves spectrogram at hectometric frequencies, and the magnetic field components and magnitude in System III coordinates. A ~2-3 day quasi-periodicity can be seen in the JEDI, JADE, and Waves data (red lines and circles). Reconnection events are highlighted in orange in the B_θ panel. The $|B|$ panel shows a gradual increase in $|B|$.

magnetosphere by solar wind shocks (Ip and Goertz, 1983). Part of our proposed work involves reduction and analysis of IoIO IPT S^+ brightness, as described in section 3.4 (Task D) below. The IPT S^+ brightness should be proportional to the square of the electron density and it is the torus species that first responds to changes in Io's atmospheric escape (e.g. Tsuchiya et al., 2019). IoIO recorded a long-term increase in the sodium nebula brightness in 2018 **(Figure 4**, right) and *preliminary* analysis of the IPT S^+ brightness suggests a delayed response similar in character.

Finally, we will augment the Juno-UVS auroral observations with HST UV auroral images collected on 94 separate dates from mid-2016 through 2018. HST images can provide an auroral context for times when Juno was in the middle and outer magnetosphere (orange dots in **Figure 3**). Grodent et al. (2018) have analyzed HST images from November 2016 through July 2017 and classified them into six auroral morphological "families" based on auroral characteristics like the total power, position and nature (e.g. narrow or broad) of the main emission, and presence or absence of injections. The different auroral "families" likely indicate different magnetospheric states or levels of activity, but to date no studies have related activity measured by Juno to changes in the auroral family classifications. We will do that here.

3. Summary of proposed research

Our work will be divided into 6 tasks, each addressing at least one motivating science question:

Task	Description	Science Question(s)
A	Measure temporal variability on short time scales	1
B	Measure current sheet variability and calculate predicted auroral shifts	1,2
C	Run SWMF-OH solar wind propagation model	1
D	Reduce and analyze IoIO images of the Io plasma torus	1,3
E	Compare in situ variability with external or internal drivers	1,3
F	Compare predicted auroral shifts and activity to Juno-UVS, HST images	2

3.1 Task A: Measuring temporal variability on short (hours to days) time scales

We will identify three types of short-term variability in Juno data as follows:

1. Transient |*B*| increases: Transient increases in $|B|$, the magnetic field magnitude, on time scales of tens of hours to days have been observed in Galileo data. Increases in $|B|$ are also known as field compressions or magnetospheric compression events, and they have been linked to both external (e.g. Hanlon et al., 2004; Tao et al., 2005) and internal drivers. Following an increase in the solar wind P_{Dyn} the subsolar distance to the magnetopause decreases from ~90 R_J to ~60 R_J (Joy et al., 2002). The reduced volume of the magnetosphere should lead to an increase in the magnetic field pressure and $|B|$ (e.g. Southwood and Kivelson, 2001). In Vogt et al. (submitted) we found a statistical link between Galileo magnetospheric compression events and increased solar wind P_{Dyn}. However, some transient $|B|$ increases occurring with a ~2-3 day quasi-periodicity have been interpreted as a magnetotail loading/unloading process associated with the internally-driven Vasyliunas cycle (Kronberg et al., 2007). Ge et al. (2007) pointed out that some lobe field $|B|$ increases occur gradually, followed by a rapid falloff, and called these events examples of an internally-driven Jovian "growth phase" because of similarities to the growth phase of terrestrial substorms. **Figure 5** shows an example of a transient $|B|$ increase featuring a gradual increase (purple) and sudden decrease (green).

We will follow the method of Vogt et al. (submitted) in surveying magnetic field data for transient increases in $|B|$ by at least a factor of 1.25 times the background lobe field, given by a local time-corrected version of the Kivelson and Khurana (2002) lobe field fit ($|B| =$

$2940 \times R^{-1.37}$ nT), where R is radial distance. We will note whether the increase in $|B|$ occurs gradually (e.g. over at least 10 hours) or occurs more suddenly.

2. Quasi-periodic modulations: Galileo data showed that quasi-periodic modulations, most often on a ~2-3 day time scale, are present in properties like the magnetic field, hectometric (HOM) auroral radio emissions, recurrence of tail reconnection events, and the energy spectral index γ (e.g., Woch et al., 1998; Kronberg et al., 2007; Vasyliunas et al., 1997; Louarn et al., 2000). The ~2-3 day quasi-periodic behavior occurs only intermittently and the characteristic period can vary from 1 to 7 days (Kronberg et al., 2009). An example of this ~2-3 day quasi-periodicity is seen in Juno JEDI, JADE, and Waves data in **Figure 5** (red lines). It is generally thought to be associated with the internal, rotationally-driven mass loading and release process of the Vasyliunas cycle. However, <u>it is not yet understood why internally-driven quasi-periodic modulations of the magnetosphere would occur intermittently or with a variable time scale</u>. We will test whether changes in the quasi-periodic behavior is affected by internal or external drivers (or both).

We will identify quasi-periodic modulations in the Juno MAG, JADE, JEDI, and Waves data. In our previous work (Vogt et al., 2010; Vogt et al., submitted) we have attempted a quantitative approach, such as calculating the Lomb periodogram of the magnetic field components, which allows one to test for statistical significance of the periodic signal. However, in our experience we have found that a quantitative approach often fails even when quasi-periodic modulations are very clearly visible. This is probably at least partly due to the fact that the modulations are <u>*quasi*</u>-periodic, with a variable period, and intermittent. Therefore, here we will again attempt a quantitative approach but will likely identify quasi-periodic behavior by eye.

3. Tail reconnection events: Magnetic reconnection is an important physical process that allows for the release of mass and energy from a planetary magnetotail. At Jupiter, tail reconnection is thought to be driven internally by the Vasyliunas cycle (Vasyliunas, 1983), in which mass-loaded flux tubes are stretched radially by the centrifugal force as they rotate into the nightside magnetotail, break, and release a plasmoid. Hundreds of reconnection events have been observed by the Galileo spacecraft in Jupiter's magnetotail (Kronberg et al., 2005; Vogt et al., 2010) with time scales of tens of minutes. Tail reconnection can be observed in magnetic field data by field dipolarizations or reversals in B_θ, the meridional magnetic field, and in particle data by radial plasma flow bursts, heating, and increased density.

In Tasks E and F we will consider the possible external or internal drivers of Juno tail reconnection events. However, we will not perform any new work to identify tail reconnection signatures since PI Vogt is funded to do so by the Juno Participating Scientist program. In her preliminary work Dr. Vogt has identified over 100 reconnection events from magnetometer data in Juno's first 14 orbits (Vogt et al., 2018), all featuring an increase in $|B_\theta|$ by a factor of ~2-3 over background levels, such as those shown in **Figure 5** (orange lines in the B_θ panel).

<u>Expected results and their significance</u>: The outputs of this task will be a list of transient $|B|$ increases and intervals when quasi-periodic behavior is observed in Juno data, and with what timescale or recurrence period. Our work will establish how variable Jupiter's magnetosphere has been on short time scales during the first ~2.5 years of the Juno mission. We will investigate possible drivers and implications of this observed variability in Tasks E and F.

3.2 Task B: Measuring current sheet variability and calculating the predicted auroral shifts

Next we will analyze changes in Jupiter's magnetosphere on long (tens of days) time scales, specifically by quantifying changes to the external (perturbation) magnetic field from orbit to orbit. The magnetic field measured by Juno in Jupiter's magnetosphere includes contributions from both the internal planetary field and the external magnetospheric currents. The internal field can be estimated from a model (e.g. the recent JRM09 model from Connerney et al., 2018, based on Juno data). Jupiter's internal field varies temporally (e.g. Moore et al., 2019), but the internal field is only a minor component of the total observed field in the middle and outer magnetosphere, and the temporal variability is only significant on time scales of years or longer. The external, or perturbation, field is primarily due to the strong azimuthal current sheet that stretches field lines radially in the middle and outer magnetosphere.

The most widely used model of Jupiter's current sheet was developed to fit the perturbation magnetic field observed during the Pioneer and Voyager flybys (Connerney et al., 1981, 1983). This model represents the current sheet as an annular disk of current, with adjustable parameters including the inner and outer edges of the disk, the disk thickness, and its current density I_0. (The current density appears in the model equations as part of the term $\mu_0 I_0$, where μ_0 is the permeability of free space). Collaborator Jack Connerney has calculated preliminary orbit-by-orbit fits to the Connerney current sheet model using magnetic field data from Juno's first 16 orbits and using JRM 09 to represent the internal field (Connerney et al., 2019). These results include a time series of the best fit $\mu_0 I_0$ term, the current sheet current density. In the analysis Dr. Connerney has specifically included an outward radial current system (Connerney, 1981), which improves the fit to the azimuthal component of the magnetic field, B_ϕ. Preliminary results of Dr. Connerney's analysis are shown in **Figure 6**. We will consult with Dr. Connerney as he finalizes his results.

After the best fit parameters are obtained we will trace model field lines, in 5 R_J increments from 10 to 150 R_J, from the equator to the ionosphere and calculate the expected ionospheric shifts in the position of the satellite footprints and expected main emission (assuming the main emission maps to, e.g. 30 R_J in the equator). An example from Vogt et al. (2017) is shown in **Figure 2**, right.

Unfortunately, as discussed in Vogt et al. (2017), the Connerney current sheet model with the default (Voyager-era) parameters breaks down for field line tracing beyond ~70 R_J, and breaks down at even smaller radial distances for larger $\mu_0 I_0$ values. If we encounter problems tracing the Connerney model field lines with the Juno fit parameters then we will fit the Juno data to the Khurana (1997) model following the method of Vogt et al. (2017). This model represents the external field with Euler potentials and accounts for features such as the field sweep back and current sheet warping and delay through 14 parameters that are fit to Pioneer and Voyager data. The largest term in the model perturbation B_Z (similar to B_θ near the equator) is $C_2 \left[\tanh \frac{\rho_{02}}{\rho}\right]^{a_2}$, where ρ is cylindrical radial distance and all other terms are fit parameters (see their eq. 21). Vogt

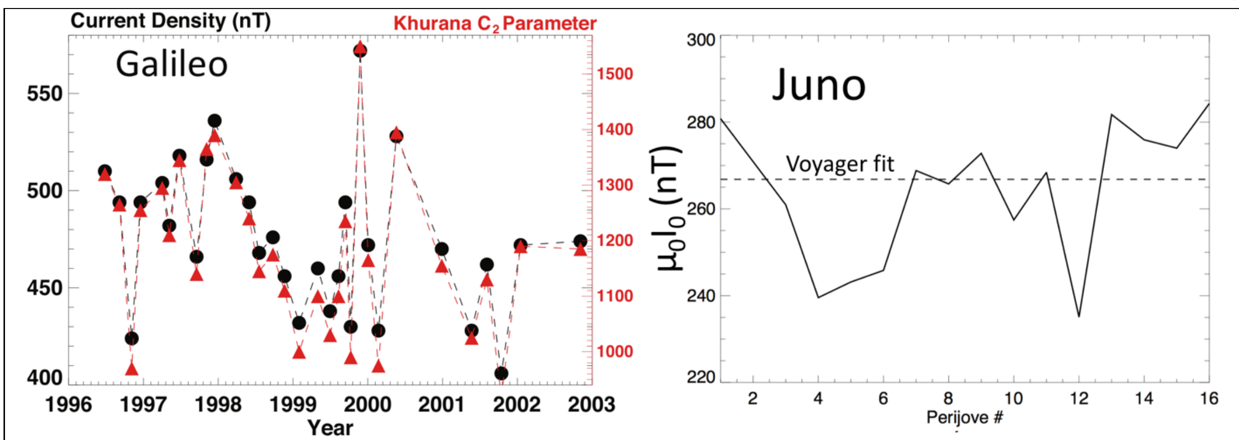

Figure 6. (left) Current sheet fit parameters to Galileo data (Vogt et al., 2017). **(right)** Preliminary best fit $\mu_0 I_0$ values from Juno's first 16 orbits from Co-I Connerney.

et al. (2017) found that varying the Khurana C_2 parameter leads to a reasonable estimate of the best fit perturbation field, and the measured variability of $\mu_0 I_0$ in the Connerney model and the Khurana C_2 parameter showed good agreement (**Figure 6**).

Expected results and their significance: The outputs of this task will include 1) a time series of the best fit current sheet parameters from a current sheet model(s), for example as shown in **Figure 6**, and 2) the predicted positions of the satellite footprints and main auroral emission obtained by tracing model field lines using the calculated best fit parameters (right panel of **Figure 2**). We will investigate possible drivers and auroral implications in Tasks E and F.

3.3 Task C: Run SWMF-OH solar wind propagation model

Measurements of the solar wind conditions upstream of Jupiter are typically not available concurrently with *in situ* magnetospheric measurements, and this continues to be the case with Juno. Therefore, we must rely on models that propagate solar wind data measured at the Earth's orbit at 1 AU out to Jupiter's orbit at 5.2 AU. The solar wind model of Tao et al. (2005) (hereafter "the Tao model") is a 1-D MHD model that propagates OMNIWeb solar wind data (model inputs are the measured solar wind mass density, velocity, magnetic field, and thermal pressure) from 1 AU out to the orbits of Jupiter and Saturn. The timing error between predicted and observed solar wind P_{Dyn} enhancements was found to be "at most 2 days" when the Earth-Sun-Ulysses angle was less than 50º. The model outputs are limited to the solar wind density, the radial component of the solar wind velocity, the solar wind speed, and one component of the IMF. Chihiro Tao is a Collaborator on this proposal and has provided PI Vogt with model outputs covering our interval of study (2016-2018). A similar 1-D MHD model, the Michigan Solar Wind Model (Zieger and Hansen, 2008), known as mSWiM, has also been widely used to predict solar wind conditions upstream of Jupiter but has not been run to cover times when Juno was in orbit around Jupiter.

In this task we will run a 2-D multi-fluid MHD solar wind propagation model, called SWMF-OH, to predict the solar wind conditions upstream of Jupiter from July 2016 through the end of 2018. A significant advantage of this model is that it can predict all three components of the interplanetary magnetic field. 1-D MHD models cannot propagate B_R because of the divergence-free nature of the magnetic field (see discussion in Zieger and Hansen, 2008). Predicting the IMF is crucial for fully understanding the interaction between the solar wind and Jupiter's magnetosphere, for example in determining whether the IMF orientation was favorable for dayside reconnection. Additionally, SWMF-OH does a good job of predicting intervals of increased solar wind P_{Dyn} from corotating interaction regions even when the Earth-Sun-Jupiter angle is large. Finally, it is useful to consider output from multiple models wherever possible, since we can have additional confidence in the predictions when results of different models agree.

SWMF-OH was adapted by Co-I Zieger from the outer heliosphere (OH) component of the Space Weather Modeling Framework (SWMF) (Tóth et al., 2012), which is a 3-D global multi-fluid MHD model of the outer heliosphere with one ion fluid and four neutral populations (Opher et al., 2006; 2009). It provides time-dependent 2-D multi-fluid MHD simulations of solar wind propagation from a heliocentric distance of 1 AU up to 50 AU. Model inputs are hourly OMNI data of the measured solar wind density, velocity, magnetic field, and temperature. Model outputs include the solar wind density, plasma temperature, velocity, and all three components of the IMF.

Co-I Zieger has used SWMF-OH to predict the conditions at Pluto and along the New Horizons trajectory. It was one of the most successful models in the New Horizons Flyby Modeling Challenge at the Community Coordinated Modeling Center (CCMC). **Figure 7** (top left) demonstrates the reasonable fit between the predicted (red) and observed (blue) solar wind speed near Pluto. The model has been successfully validated with Pioneer 10 and Voyager 2 data (**Figure 7**, bottom left). **Preliminary results of solar wind propagation to Juno during its cruise phase to Jupiter (Moore et al., 2017), shown in Figure 7, demonstrate that not only the plasma parameters but also the interplanetary magnetic field (IMF) can be reasonably well predicted with the SWMF-OH at Jupiter's orbit.** The expected timing errors have not yet been quantified, but we will do so using the Juno cruise data, and anticipate that they will be roughly similar to mSWiM (10-15 hours for high recurrence index, ~35 hours for a low recurrence index).

The SWMF-OH model will be run on the NASA Pleiades supercomputer at the NASA Advanced Supercomputing (NAS) facility at NASA Ames. The model takes about a week to provide one entire year of propagated solar wind data. If we encounter unexpected problems running SWMF-OH then Co-I Zieger will run the mSWiM model for 2016-2018. mSWiM can be run on a desktop computer in a few days.

Expected results and their significance: We will produce new SWMF-OH predictions of the solar wind conditions upstream of Jupiter from mid-2016 through the end of 2018. SWMF-OH provides an improvement on other available models because it predicts all three components of the IMF. **The predicted solar wind conditions upstream of Jupiter will be useful beyond just the work described in this proposal, and will help provide context for other studies of Juno data.** We will share the solar wind propagation model results with members of the Juno team and with other members of the community as soon as possible via our website.

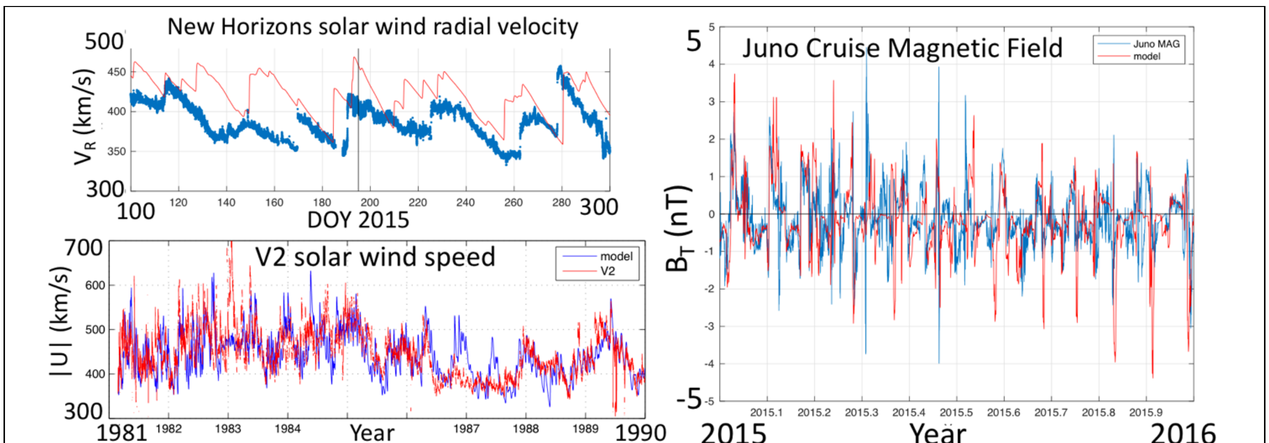

Figure 7. (top left) Predicted (red) and observed (blue) solar wind speed at New Horizons during the Pluto Flyby. **(bottom left)** Predicted (blue) and observed (red) solar wind speed at Voyager 2. **(right)** Predicted (red) and Juno MAG data (blue) during Juno's approach of Jupiter in 2015.

3.4 Task D: Reduce and analyze IoIO images of the Io plasma torus

In this task we will reduce and analyze IoIO images to provide a long-term measurement of the IPT, which we will use to help interpret the how internal drivers affect the temporal variability measured in Jupiter's magnetosphere in Tasks A and B. IPT images recorded by IoIO (**Figure 4**) are of sufficient quality to extract the IPT S^+ brightness and its dawn-dusk displacement. **Figure 4** (right) shows a first analysis of the IoIO sodium (left) and IPT (right) data using simple wide-field aperture sums. The technique of using concentric apertures applied by Morgenthaler et al. (2019) is adequate for the sodium nebula but needs modification to track the small and dynamic torus S^+ ribbon. We will analyze the IoIO [SII] 6731 Å IPT images here.

The work of reducing the IoIO IPT images is straightforward: an accurate center for Jupiter must be found for each image. Using the positions of Galilean satellites as a guide, the rotational orientation of each image must be corrected (< 3° effect). Then, using a boxcar search algorithm with various sized boxes, the astrometric center of each ansa (edge) will be found and the vertical and horizontal extent of the ansas measured. Finally, the average surface brightness of each ansa, calculated for a range of box sizes will be tabulated. All these results will be added to a CSV file which summarizes the reduction and analysis results. A first version of that file was published as supplemental material to Morgenthaler et al. (2019), which focused exclusively on sodium nebula measurements. Any improved versions of that file will be published with results using the data.

Finally, we will use Juno radio occultation data, which measures IPT densities (TECs), to confirm the expected relationship between IPT densities and IoIO S^+ brightness measurements and to provide coverage prior to IoIO's commissioning in 2017. IoIO data are available at and around the times of Juno's PJ 11 (7 Feb. 2018) and 13 (24 May 2018), when radio occultations of the IPT are also available. IoIO data are available for three days following PJ 6 (19 May 2017).

Expected results and their significance: The outputs of this task will include a time series of the nightly median of IPT brightness over our interval of study, similar to the IoIO sodium nebula brightness shown in **Figure 4**, and a time series of the dawn-dusk displacement of the IPT. **Like the output of our solar wind model runs, these results will have impact beyond just the work proposed here, for they will help provide context for any study that uses Juno data.**

3.5 Task E: Compare **in situ** *variability with external or internal drivers*

In Tasks A and B we will have established when Juno observed temporal variability in Jupiter's middle and outer magnetosphere, such as quasi-periodic modulations of the magnetic field and other properties and tail reconnection signatures, and the long-term variability of Jupiter's current sheet. Here we will compare this variability to the SWMF-OH modeled solar wind conditions obtained in Task C and the ground-based Io plasma torus observations reduced and analyzed in Task D, to determine the relative roles of external and internal drivers. (We will consider both SWMF-OH and Tao model solar wind output but will focus on SWMF-OH.)

Much of our work will proceed qualitatively. For example, for each type of variability considered in Tasks A and B we will determine whether it is typically associated with particular conditions in the modeled solar wind (such as enhanced P_{Dyn} or a particular IMF direction) or increased activity from Io as indicated by enhanced IPT S^+ brightness. We will establish whether the "growth phase" gradual $|B|$ increase events are indeed associated internal driving as expected (Ge et al., 2007). We will test the predictions that tail reconnection signatures and solar wind-induced magnetospheric compressions should be accompanied by substantial dawn-dusk displacements of the IPT (Barbosa and Kivelson, 1983; Brown and Bouchez, 1997; Ip and Goertz, 1983). Additionally, our analysis will provide the first opportunity for direct observational evidence that increased IPT activity is linked to magnetotail reconnection. We will also determine whether Juno orbits with an especially weak or strong current sheet (e.g. from the $\mu_0 I_0$ fit) were associated with noteworthy IPT or solar wind conditions. Finally, we will consider whether tail reconnection events or transient $|B|$ increases are associated with a particular IMF orientation that favors dayside reconnection (e.g. Desroche et al., 2012; Masters, 2017) and enables addition of open flux to the magnetosphere.

Where appropriate, we will also perform quantitative analyses to test for a statistical link between changes in Jupiter's magnetosphere and external or internal drivers. For example, we will follow Vogt et al. (submitted) in performing an event association test (e.g. Hsu and McPherron, 2002), which is similar to a cross-correlation but is calculated for event timings, to determine whether increases in the predicted solar wind P_{Dyn} can be statistically associated with events identified in Task A. We will also look for any quasi-periodic signals in the predicted solar wind velocity and IMF that could explain the quasi-periodic modulations in Jupiter's magnetosphere.

Expected results and their significance: The results of this task will include both qualitative and quantitative assessments of the association between magnetospheric variability observed by Juno and variability in two likely drivers, the solar wind and the Io plasma torus. Our findings will contribute to our understanding of the sources of temporal variability in Jupiter's magnetosphere. **Our results will provide the first long-term comparison between ground-based IPT observations and in situ measurements from Jupiter's magnetosphere.** This comparison will help establish the timescales over which changes in the IPT influence the magnetosphere. We will determine whether tail reconnection events are influenced by increases in the IPT density. This will contribute to our understanding of the role that tail reconnection plays in the overall magnetospheric mass and energy transport, which remains a topic of debate (e.g. Vogt et al., 2014; Cowley et al., 2015), since increased Io plasma production requires additional mass output from the system, which could be achieved either through plasmoid release or other processes.

3.6 Task F: Compare predicted auroral shifts and activity to Juno UVS and HST images

In this Task we will compare the predicted auroral shifts from Task B to the observed auroral positions measured with Juno UVS and HST. Collaborator Greathouse will provide the location of the main auroral emission in Juno UVS images (Greathouse et al., 2019) for each PJ (except for PJ2 when Juno went into safe mode), and Collaborator Grodent will provide the location of the main auroral images in HST images, along with auroral "family" designations. **Figure 8** shows Juno UVS auroral images from PJ 12, for which the main auroral emission was significantly compressed, or poleward, compared to its typical location, and PJ 13, for which the main auroral emission was significantly expanded, or equatorward. Though the Juno UVS images are not concurrent with the MAG data that provided the current sheet fitting, they are close in time (separated by at most 4 days) since the current sheet fits will be performed when Juno is close to Jupiter ($R < \sim 50\ R_J$). Some HST images are exactly concurrent with the magnetic field data.

For each Juno perijove or date with HST images we will qualitatively compare the position of the main emission to reference ovals (e.g. Nichols et al., 2009) to determine whether the aurora is in a compressed, expanded, or typical state. We will also calculate the average displacement between the observed main emission location and a reference oval, and correlate this displacement with the best fit current sheet parameters from Task B. If we assume that the CEC system that drives the main auroral emission is fixed in radial distance, we expect orbits with larger $\mu_0 I_0$ (more stretched field) will feature a more expanded main emission and vice-versa (e.g. **Figure 2**, right). If we find little or no quantitative or qualitative relationship between the main emission location

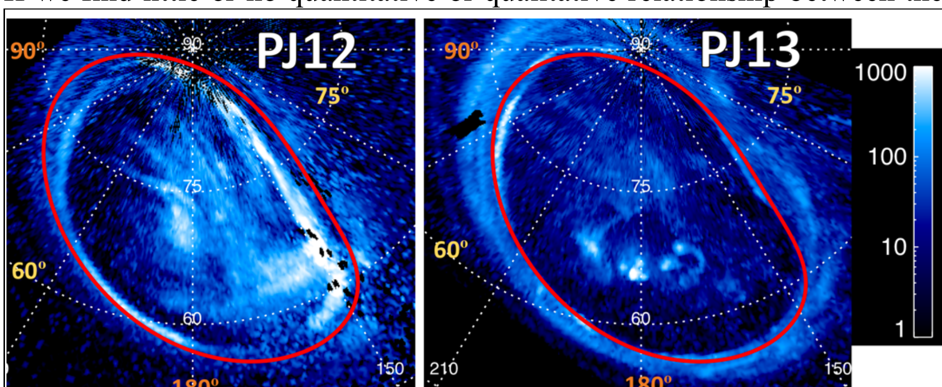

Figure 8. Juno UVS images of Jupiter's northern aurora for PJ 12 (compressed main emission) and PJ 13 (expanded). The red line shows the JRM09 Callisto footprint path.

and $\mu_0 I_0$ or C_2 then we can conclude that the CEC system that drives the main auroral emission is not fixed in radial distance. We can then trace field lines or use the Vogt et al. (2011, 2015) flux mapping to estimate the radial mapping of the main auroral emission in the equator, which provides insight into variability in Jupiter's magnetosphere-ionosphere coupling system.

Finally, we will determine whether there is a relationship between the Grodent et al. (2018) auroral "family" designations for HST images and any concurrent magnetospheric activity identified in Task A. For example, we will examine whether the "injection" or "strong injection" family of images typically occur near times that Juno observed tail reconnection signatures, as expected (e.g. Louarn et al., 2014). We will also determine whether the "external perturbation" family of images, which Grodent et al. (2018) suggested is caused by a solar wind-driven magnetospheric compression event, occurred during times of high predicted solar wind P_{Dyn}.

Expected results and their significance: The results of this task will include scatter plots of the displacement of the main emission as a function of the best fit current sheet parameter. We will also link auroral "family" designations to magnetospheric activity observed *in situ* by Juno. Our findings will establish how temporal variability in Jupiter's magnetosphere affects the location and morphology of Jupiter's aurora.

4. Research Team and Work Plan

PI Marissa Vogt will advise a Boston University graduate student, who will be responsible for the bulk of the proposed work, and will manage the contributions from other team members. Dr. Vogt is a Juno Participating Scientist (PS) and therefore is familiar with the Juno data and has access to Juno analysis and plotting tools that will facilitate the work described here. Dr. Vogt will be responsible for the management of this investigation, compliance with all reporting requirements, and implementation of the data management plan. Finally, Dr. Vogt will provide a list of tail reconnection signatures identified from Juno magnetometer data, which will be supported by her Juno PS work (no effort requested here). Dr. Vogt will manage team member contributions through in-person meetings during regular Juno science team meetings and other conferences, and emails or telecons as necessary. Her level of effort will be 1 month per year.

A Boston University Graduate Student will perform the data analysis, modeling work, and other calculations described in Tasks A, B, E, and F. The work described in these tasks are highly complementary to previous work led by PI Vogt using Galileo data (Vogt et al., 2017; Vogt et al., submitted) and so the work should be relatively straightforward and appropriate for a graduate student. The student will also present intermediate results at conferences, will be responsible for preparing manuscripts for publication, and will assist with implementation of the data management plan. The student's level of effort will be 9 months per year (0.75 FTE).

Co-I Bertalan Zieger will run the SWMF-OH model to predict the solar wind conditions upstream of Jupiter during Juno's first ~2.5 years in Jovian orbit (Task C). Co-I Zieger was the lead author of the mSWiM 1-D MHD solar wind propagation model for conditions upstream of Jupiter and Saturn (Zieger and Hansen, 2008). His level of effort will be 1 month per year.

Co-I Jeff Morgenthaler will reduce and analyze IoIO images of S^+ in the IPT. As discussed in the PSI subcontract Statement of Work, this task was descoped from the original IoIO NSF-funded project because that project was funded only at the 40% level. Because the IPT measurements are critical to our work, this task must be funded as part of our requested effort if the work is to succeed within the budgeted timeframe. His level of effort will be 1 month per year.

Collaborator Paul Withers and Co-I Phillip Phipps will consult on variability of the Io plasma torus as measured by Juno radio occultations. Co-I Phipps will provide TEC profiles and peak TEC values for PJs 1, 3, 6, and 8 (Phipps et al., 2018, 2019) and for PJs 10, 11, 13, 14, and 15 based on analysis of data publicly available on the PDS. No funded effort is requested for Drs. Withers or Phipps as they will be supported by an existing NFDAP award to Dr. Withers.

Collaborator Jack Connerney will provide best fit parameters to the external magnetic field measured by Juno. No funded effort is requested because Dr. Connerney's contribution falls within his role as a member of the Juno team and MAG instrument lead.

Collaborator Thomas Greathouse will provide Juno UVS observations of the variability in the main auroral emission position (Figure 8). No funded effort is requested because Dr. Greathouse's contribution falls within his role as a member of the Juno-UVS team.

Collaborator Denis Grodent will provide the position of the main auroral emission for HST images and auroral "family" designations. He has already published the auroral "family" designations for HST images through July 2017 (Grodent et al., 2018).

Collaborator Chihiro Tao will consult on the interpretation of the Tao model predicted solar wind conditions upstream of Jupiter and has already provided model outputs for 2016-2018.

Our work plan is summarized in the following table. In all Years PI Vogt will advise the graduate student and manage the overall progress of the work in this proposal (1 month per year).

Year	Description
1	**Graduate student:** perform Task A (6 months), perform Task B (3 months) **Co-I Zieger:** begin running the SWMF-OH model (1 month) **Co-I Morgenthaler:** begin reducing and analyzing IoIO data (1 month)
2	**Graduate student:** perform Task F (6 months), prepare publication (3 months) **Co-I Zieger:** continue running the SWMF-OH model, prepare publication (1 month) **Co-I Morgenthaler:** continue analyzing IoIO data, prepare publication (1 month)
3	**Graduate student:** perform Task E (6 months), prepare publication (3 months) **Co-I Zieger:** finalize model output and publication, consult with graduate student in interpreting results (1 month) **Co-I Morgenthaler:** finalize IoIO analysis and publication, consult with graduate student in interpreting results (1 month)

We will publish 4 peer-reviewed manuscripts: one presenting Juno observations of temporal variability in the magnetosphere and likely drivers (Tasks A and E), one comparing the Juno UVS and HST auroral variability with the current sheet fitting (Tasks B and F), one covering the solar wind modeling results (Task C), and one discussing the IoIO data (Task D).

5. Statement of non-overlap with Juno mission activities and funding

PI Marissa Vogt currently receives funding from the NASA Juno Participating Scientist program. Dr. Vogt's funded responsibilities as a member of the Juno science team are limited to the tasks described in her Juno PS proposal, which are, broadly, 1) identify reconnection events in Juno data and 2) quantify the mass lost and flux closed by plasmoids. <u>The work described in that proposal does not include analysis of solar wind models or IPT data.</u> Therefore the scientific objectives and the work described here do not overlap in scope with Dr. Vogt's submitted Juno PS proposal, available at http://sites.bu.edu/marissavogt/files/2019/07/vogt_juno_ps_2018_STM.pdf All other Juno team members included in this proposal are participating as unfunded collaborators. Additionally, there is very little overlap between our work on the middle and outer magnetosphere and ongoing Juno team activities, which have largely been focused on Juno's polar magnetosphere (see list maintained at http://lasp.colorado.edu/home/mop/bibliographies/juno-science-papers/).

References

Asmar, S.W., et al. (2017), The Juno Gravity Science Instrument, Space Science Reviews, 213, 205-218, doi:10.1007/s11214-017-0428-7.

Barbosa, D. D., & Kivelson, M. G., Dawn-dusk electric field asymmetry of the Io plasma torus, Geophys. Res. Lett., Vol. 10, p. 210-213, 1983.

Behannon, K. W., L. F. Burlaga, and N. F. Ness (1981), The Jovian magnetotail and its current sheet, J. Geophys. Res., 86, 8385-8401.

Bolton, S.J., Lunine, J., Stevenson, D. et al. Space Sci Rev (2017) 213: 5. https://doi.org/10.1007/s11214-017-0429-6

Brown, M. E. and A. H. Bouchez (1997), The Response of Jupiter's Magnetosphere to an Outburst on Io, Science, 278 (5336), 268-271, doi:10.1126/science.278.5336.268

Connerney, J. E. P. (1981), Comment on ‘Azimuthal magnetic field at Jupiter' by J. L. Parish, C. K. Goertz, and M. F. Thomsen, J. Geophys. Res., 86(A9), 7796– 7797, doi:10.1029/JA086iA09p07796.

Connerney, J. E. P., Kotsiaros, S., Oliversen, R. J., Espley, J. R., Joergensen, J. L., Joergensen, P. S., et al. (2018). A new model of Jupiter's magnetic field from Juno's first nine orbits. Geophysical Research Letters, 45.

Connerney, J. E. P., M. H. Acuña, and N. F. Ness (1983), Currents in Saturn's magnetosphere, J. Geophys. Res., 88, 8779–8789.

Connerney, J., M. Acuña, and N. Ness (1981), Modeling the Jovian Current Sheet and Inner Magnetosphere, J. Geophys. Res., 86(A10), 8370-8384.

Connerney, J.E.P., Benn, M., Bjarno, J.B. et al. (2017), The Juno Magnetic Field Investigation, Space Sci Rev 213: 39. https://doi.org/10.1007/s11214-017-0334-z

Connerney, J. E. P., S. Kotsiaros, D. Gershman, Y. Martos, J. L. Joergensen, J. M. G. Merayo, M. Herceg, S. J. Bolton, and S. M Levin (2019), Jupiter’s Magnetosphere at the Midpoint of Juno’s Mapping Mission, Magnetospheres of the Outer Planets abstracts, Sendai, Japan, June 2019 (http://pparc.tohoku.ac.jp/sympo/mop/wp-content/uploads/2019/05/MOP2019_program_book.pdf).

Cowley, S. W. H., and E. J. Bunce (2001), Origin of the main auroral oval in Jupiter’s coupled magnetosphere-ionosphere system, Plan. Space Sci., 49, 1067-1088.

Cowley, S. W. H., and E. J. Bunce (2003a), Modulation of Jovian middle magnetosphere currents and auroral precipitation by solar wind-induced compressions and expansions of the magnetosphere: initial response and steady state, Planet. Space Sci., 51, 31-56.

Cowley, S. W. H., and E. J. Bunce (2003b), Modulation of Jupiter's main auroral oval emissions by solar wind induced expansions and compressions of the magnetosphere, Planet. Space Sci., 51, 57-79.
Cowley, S. W. H., Nichols, J. D., and Jackman, C. M. (2015), Down-tail mass loss by plasmoids in Jupiter's and Saturn's magnetospheres, J. Geophys. Res. Space Physics, 120, 6347– 6356, doi:10.1002/2015JA021500.

Cowley, S. W. H., S. V. Badman, S. M. Imber, and S. E. Milan (2008), Comment on "Jupiter: A fundamentally different magnetospheric interaction with the solar wind" by D. J. McComas and F. Bagenal, Geophys. Res. Lett., 35, L101010, doi:10.1029/2007GL032645.

Delamere, P. A. and F. Bagenal (2003), Modeling variability of plasma conditions in the Io torus, J. Geophys. Res., 108, A7, doi:10.1029/2002JA009706.

Delamere, P. A., and F. Bagenal (2010), Solar wind interaction with Jupiter's magnetosphere, J. Geophys. Res., 115, A10201, doi:10.1029/2010JA015347.

Desroche, M., F. Bagenal, P. A. Delamere, and N. Erkaev (2012), Conditions at the expanded Jovian magnetopause and implications for the solar wind interaction, J. Geophys. Res., 117, A07202, doi:10.1029/2012JA017621.

Ge, Y. S., L. K. Jian, and C. T. Russell (2007), Growth phase of Jovian substorms, Geophys. Res. Lett., 34, L23106, doi:10.1029/2007GL031987.

Gladstone, G.R., Persyn, S.C., Eterno, J.S. et al. (2014), The Ultraviolet Spectrograph on NASA's Juno Mission, Space Sci. Rev., 213: 447. https://doi.org/10.1007/s11214-014-0040-z

Greathouse, T. K., G. R. Gladstone, M. H. Versteeg, V. Hue, J. A. Kammer, M. W. Davis, S. J. Bolton, S. Levin, J. E. P. Connerney, J.-C. Gérard, D. Grodent, B. Bonfond, and E. J. Bunce (2019), A study of Local Time Variations of Jupiter's Ultraviolet Aurora using Juno UVS, Magnetospheres of the Outer Planets abstracts, Sendai, Japan, June 2019 (http://pparc.tohoku.ac.jp/sympo/mop/wp-content/uploads/2019/05/MOP2019_program_book.pdf).

Grodent, D., Bonfond, B., Yao, Z., Gérard, J.-C., Radioti, A., Dumont, M., et al. (2018). Jupiter's aurora observed with HST during Juno orbits 3 to 7. Journal of Geophysical Research: Space Physics, 123, 3299– 3319. https://doi.org/10.1002/2017JA025046

Grodent, D., J.-C. Gérard, A. Radioti, B. Bonfond, and A. Saglam (2008), Jupiter's changing auroral location, J. Geophys. Res., 113, A01206, doi:10.1029/2007JA012601.

Gurnett, D. A., W. S. Kurth, G. B. Hospodarsky, A. M. Persoon, P. Zarka, A. Lecacheux, S. J. Bolton, M. D. Desch, W. M. Farrell, M. L. Kaiser, H.-P. Ladreiter, H. O. Rucker, P. Galopeau, P. Louarn, D. T. Young, W. R. Pryor, and M. K. Dougherty (2002), Control of Jupiter's radio emission and aurorae by the solar wind, Nature, 415, 985-987.

Hanlon, P. G., M. K. Dougherty, N. Krupp, K. C. Hansen, F. J. Crary, D. T. Young, and G. Tóth (2004), Dual spacecraft observations of a compression event within the Jovian magnetosphere: Signatures of externally triggered supercorotation?, J. Geophys. Res., 109, A09S09, doi:10.1029/2003JA010116.

Hill, T. W. (2001), The Jovian auroral oval, J. Geophys. Res., 106, 8101-8107.

Hsu., T.-S., and R. L. McPherron (2002), An evaluation of the statistical significance of the association between northward turnings of the interplanetary magnetic field and substorm onsets, J. Geophys. Res., 107(A11), 1398, doi:10.1029/2000JA000125.

Ip, W.-H., & Goertz, C. K., An interpretation of the dawn-dusk asymmetry of UV emission from the Io plasma torus, Nature, Vol. 302, p. 232, 1983.

Joy, S. P., M. G. Kivelson, R. J. Walker, K. K. Khurana, C. T. Russell, and T. Ogino (2002), Probabilistic models of the Jovian magnetopause and bow shock locations, J. Geophys. Res., 107, 1309, doi: 10.1029/2001JA009146.

Khurana, K. K. (1997), Euler potential models of Jupiter's magnetospheric field, J. Geophys. Res., 102(A6), 11295-11306.

Kimura, T., et al. (2017), Transient brightening of Jupiter's aurora observed by the Hisaki satellite and Hubble Space Telescope during approach phase of the Juno spacecraft, Geophys. Res. Lett., 44, 4523– 4531, doi:10.1002/2017GL072912.

Kivelson, M. G., and K. K. Khurana (2002), Properties of the magnetic field in the Jovian magnetotail, J. Geophys. Res., 107(A8), 1196.

Kronberg, E. A., J. Woch, N. Krupp, A. Lagg, K. K. Khurana, and K.-H. Glassmeier (2005), Mass release at Jupiter: Substorm-like processes in the Jovian magnetotail, J. Geophys. Res., 110, A03211, doi:10.1029/2004JA010777.

Kronberg, E. A., J. Woch, N. Krupp, and A. Lagg (2008), Mass release process in the Jovian magnetosphere: Statistics on particle burst parameters, J. Geophys. Res., doi:10.1029/2008JA013332.

Kronberg, E. A., J. Woch, N. Krupp, and A. Lagg (2009), A summary of observational records on periodicities above the rotational period in the Jovian magnetosphere, Ann. Geophys., 27, 2565-2573.

Kronberg, E. A., K.-H. Glassmeier, J. Woch, N. Krupp, A. Lagg, and M.K. Dougherty (2007), A possible intrinsic mechanism for the quasi-periodic dynamics of the Jovian magnetosphere, J. Geophys. Res., 112, A05203, doi:10.1029/2006JA011994.

Kurth, W.S., et al. (2017), The Juno Waves Investigation, Space Science Reviews, 213, 347-392, doi:10.1007/s11214-017-0396-y.

Louarn, P., A. Roux, S. Perraut, W. Kurth, and D. Gurnett (1998), A study of the large-scale dynamics of the Jovian magnetosphere using the Galileo Plasma Wave Experiment, Geophys. Res. Lett., 25, 2905-2908.

Louarn, P., A. Roux, S. Perraut, W. S. Kurth, and D. A. Gurnett (2000), A study of the Jovian "energetic magnetospheric events" observed by Galileo: role in the radial plasma transport, J. Geophys. Res., 105, 13073-13088.

Louarn, P., C. P. Paranicas, and W. S. Kurth (2014), Global magnetodisk disturbances and energetic particle injections at Jupiter, J. Geophys. Res. Space Physics, 119, 4495–4511, doi:10.1002/2014JA019846.

Louarn, P., W. S. Kurth, D. A. Gurnett, G. B. Hospodarsky, A. M. Persoon, B. Cecconi, A. Lecacheux, P. Zarka, P. Canu, A. Roux, H. O. Rucker, W. M. Farrell, M. L. Kaiser, N. Andre, C. Harvey, and M. Blanc (2007), Observation of similar radio signatures at Saturn and Jupiter: Implications for the magnetospheric dynamics, Geophys. Res. Lett., 34, L20113, doi:10.1029/2007GL030368.

Masters, A. (2017). Model-based assessments of magnetic reconnection and Kelvin-Helmholtz instability at Jupiter's magnetopause. Journal of Geophysical Research: Space Physics, 122, 11,154–11,174. https://doi.org/10.1002/ 2017JA024736

Mauk, B.H., Haggerty, D.K., Jaskulek, S.E. et al. (2017), Space Sci Rev, 213: 289. https://doi.org/10.1007/s11214-013-0025-3

McComas, D. J., and F. Bagenal (2007), Jupiter: A fundamentally different magnetospheric interaction with the solar wind, Geophys. Res. Lett., 34, L20106, doi:10.1029/2007GL031078.

McComas, D.J., et al. (2017), The Jovian Auroral Distributions Experiment (JADE) on the Juno Mission to Jupiter, Space Science Reviews, 213, 547-643, doi:10.1007/s11214-013-9990-9.

Mendillo, M., J. Baumgardner, B. Flynn, and J. Hughes (1990), The extended sodium nebula of Jupiter, Nature, 348, 312–314.

Mendillo, M., J. Wilson, J. Spencer, and J. Stansberry (2004), Io's volcanic control of Jupiter's extended neutral clouds, Icarus, 170, 430-442.

Moore, L., J. O'Donoghue, H. Melin, T. Stallard, C. Tao, B. Zieger, J. Clarke, M. F. Vogt, T. Bhakyapaibul, M. Opher, G. Tóth, J. E. P. Connerney, S. Levin, and S. Bolton (2017), Variability of Jupiter's IR H3+ aurorae during Juno approach, Geophys. Res. Lett., 44, 4513–4522, doi:10.1002/2017GL073156.

Moore, K. M., H. Cao, J. Bloxham, D. J. Stevenson, J. E. P. Connerney, and S. J. Bolton. 2019. "Time variation of Jupiter's internal magnetic field consistent with zonal wind advection." Nature Astronomy. doi:10.1038/s41550-019-0772-5.

Morgenthaler, J. P., Rathbun, J. A., Schmidt, C. A., Baumgardner, J., & Schneider, N. M., Large Volcanic Event on Io Inferred from Jovian Sodium Nebula Brightening, Astrophys. J., Lett., Vol. 871, No. 2, p. L23, 2019.

Nichols, J. D. (2011), Magnetosphere-ionosphere coupling in Jupiter's middle magnetosphere: Computations including a self-consistent current sheet magnetic field model, J. Geophys. Res., 116, A10232, doi:10.1029/2011JA016922.

Nichols, J. D. and S. W. H. Cowley (2004), Magnetosphere-ionosphere coupling currents in Jupiter's middle magnetosphere: effect of precipitation-induced enhancement of the ionospheric Pedersen conductivity, Ann. Geophys., 22, 1799-1827, doi:10.5194/angeo-22-1799-2004.

Nichols, J. D., J. T. Clarke, J. C. Gérard, D. Grodent, and K. C. Hansen (2009), Variation of different components of Jupiter's auroral emission, J. Geophys. Res., 114, A06210, doi:10.1029/2009JA014051.

Nichols, J. D., N. Achilleos, and S. W. H. Cowley (2015), A model of force balance in Jupiter's magnetodisc including hot plasma pressure anisotropy, J. Geophys. Res. Space Physics, 120, 10,185–10,206, doi:10.1002/2015JA021807.

Nozawa, H., H. Misawa, S. Takahashi, A. Morioka, S. Okano, and R. Sood (2005), Relationship between the Jovian magnetospheric plasma density and Io torus emission, Geophys. Res. Lett., 32, L11101, doi:10.1029/2005GL022759.

Opher, M. et al., Astrophys. J. Lett., 640, L71-L74, 2006.

Opher, M. et al., Nature, 462, 1036-1038, 2009.

Phipps and Withers (2017), Radio occultations of the Io plasma torus by Juno are feasible, J. Geophys. Res. Space Physics, 122, DOI:10.1002/2016JA023447

Phipps et al. (2018), Distribution of Plasma in the Io Plasma Torus as Seen by Radio Occultation During Juno Perijove 1, J. Geophys. Res. Space Physics, 123, DOI:10.1029/2017JA025113

Phipps, P. H., Withers, P., Buccino, D. R., Yang, Y.-M., & Parisi, M. (2019). Variations in the density distribution of the Io plasma torus as seen by radio occultations on Juno Perijoves 3, 6, and 8. Journal of Geophysical Research: Space Physics, 124. https://doi.org/10.1029/2018JA026297

Rathbun, J. A., J. R. Spencer, A. G. Davies, R. R. Howell, and L. Wilson (2002), Loki, Io: A periodic volcano, Geophys. Res. Lett., 29(10), 1443, doi:10.1029/2002GL014747.

Russell, C. T., Z. J. Yu, K. K. Khurana, and M. G. Kivelson (2001), Magnetic field changes in the inner magnetosphere of Jupiter, Adv. Space Res., 28(6), 897-902.

Smith, E. J., L. Davis Jr., D. E. Jones, P. J. Coleman Jr., D. S. Colburn, P. Dyal, C. P. Sonett, and A. M. A. Frandsen (1974), The planetary magnetic field and magnetosphere of Jupiter: Pioneer 10, J. Geophys. Res., 79(25), 3501–3513, doi:10.1029/JA079i025p03501.

Southwood, D. J., and M. G. Kivelson (2001), A new perspective concerning the influence of the solar wind on the Jovian magnetosphere, J. Geophys. Res., 106(A4), 6123-6130.

Tao, C., R. Kataoka, H. Fukunishi, Y. Takahashi, and T. Yokoyama (2005), Magnetic field variations in the Jovian magnetotail induced by solar wind dynamic pressure enhancements, J. Geophys. Res., 110, A11208, doi:10.1029/2004JA010959.

Thomas, N., G. Lichtenberg, and M. Scotto, High-resolution spec- troscopy of the Io plasma torus during the Galileo mission, J. Geophys. Res. 106, 26,277–26,292, 2001.

Thomas, N., F. Bagenal, T. W. Hill, and J. K. Wilson (2004), in Jupiter: the Planet, Satellites, and Magnetosphere, edited by F. Bagenal et al., Cambridge Univ. Press, New York.

Tóth, G. et al., J. Comp. Phys., 231, 870-903, 2012.

Tsuchiya, F., Yoshioka, K., Kimura, T., Koga, R., Murakami, G., Yamazaki, A., et al. (2018). Enhancement of the Jovian magnetospheric plasma circulation caused by the change in plasma supply from the satellite Io. Journal of Geophysical Research: Space Physics, 123, 6514– 6532. https://doi.org/10.1029/2018JA025316

Tsuchiya, F., Arakawa, R., Misawa, H., Kagitani, M., Koga, R., Suzuki, F., et al. (2019). Azimuthal variation in the Io plasma torus observed by the Hisaki satellite from 2013 to 2016. Journal of Geophysical Research: Space Physics, 124, 3236– 3254. https://doi.org/10.1029/2018JA026038

Vasyliūnas, V. M. (1983), Plasma distribution and flow, in Physics of the Jovian Magnetosphere, edited by A. J. Dessler, p. 395, Cambridge Univ. Press, New York.

Vasyliūnas, V. M., Frank, L. A., Ackerson, K. L., and Paterson, W. R. (1997), Geometry of the plasma sheet in the midnight-to-dawn sector of the Jovian magnetosphere: Plasma observations with the Galileo spacecraft, Geophys. Res. Lett., 24, 869–872.

Vogt, M. F., M. G. Kivelson, K. K. Khurana, S. P. Joy, and R. J. Walker (2010), Reconnection and flows in the Jovian magnetotail as inferred from magnetometer observations, J. Geophys. Res., 115, A06219, doi: 10.1029/2009JA015098.

Vogt, M. F., M. G. Kivelson, K. K. Khurana, R. J. Walker, B. Bonfond, D. Grodent, and A. Radioti (2011), Improved mapping of Jupiter's auroral features to magnetospheric sources, J. Geophys. Res., 116, A03220, doi:10.1029/2010JA016148.

Vogt, M. F., C. M. Jackman, J. A. Slavin, E. J. Bunce, S. W. H. Cowley, M. G. Kivelson, and K. K. Khurana (2014), Structure and Statistical Properties of Plasmoids in Jupiter's Magnetotail, J. Geophys. Res. Space Physics, 119, 821-843, doi:10.1002/2013JA019393.

Vogt, M. F., E. J. Bunce, M. G. Kivelson, K. K. Khurana, R. J. Walker, A. Radioti, B. Bonfond, and D. Grodent (2015), Magnetosphere-ionosphere mapping at Jupiter: Quantifying the effects of using different internal field models, J. Geophys. Res. Space Physics, 120, 2584–2599,

Vogt, M. F., E. J. Bunce, J. D. Nichols, J. T. Clarke, and W. S. Kurth (2017), Long-term variability of Jupiter's magnetodisk and implications for the aurora, Journal of Geophysical Research: Space Physics, 122, 12,090–12,110, doi:10.1002/2017JA024066. doi:10.1002/2014JA020729.

Vogt, M. F.; Thomsen, M. F.; Ebert, R. W.; Wilson, R. J.; Allegrini, F.; Connerney, J. E. P.; DiBraccio, G. A.; Gershman, D. J.; Clark, G. B.; Paranicas, C.; Kurth, W. S.; and Valek, P. W. (2018), Magnetotail Reconnection at Jupiter: A survey of magnetic field and plasma flow signatures observed by Juno, American Geophysical Union, Fall Meeting 2018, abstract #SM23G-3265.

Vogt, M. F., S. Gyalay, E. A. Kronberg, E. J. Bunce, W. S. Kurth, B. Zieger, and C. Tao, Solar wind interaction with Jupiter's magnetosphere: A statistical study of Galileo in situ data and modeled upstream solar wind conditions, submitted to J. Geophys. Res - Space Physics, in revision, 2019.

Wilson, J. K., Mendillo, M., Baumgardner, J., et al. (2002), The Dual Sources of Io's Sodium Clouds, Icarus, 157, 476, doi:10.1006/icar.2002.6821

Woch, J., N. Krupp, A. Lagg, B. Wilken, S. Livi, and D. J. Williams (1998), Quasi-periodic modulations of the Jovian magnetotail, Geophys. Res. Lett., 25, 1253-1256, doi:10.1029/98GL00861.

Woch, J., N. Krupp, A. Lagg, B. Wilken, S. Livi, and D. J. Williams (1998), Quasi-periodic modulations of the Jovian magnetotail, Geophys. Res. Lett., 25, 1253.

Yoneda, M., Kagitani, M., Tsuchiya, F., Sakanoi, T., & Okano, S. (2015), Brightening event seen in observations of Jupiter's extended sodium nebula, Icarus, 261, 31, doi: 10.1016/j.icarus.2015.07.037

Zieger , B. and K. C. Hansen (2008), Statistical validation of a solar wind propagation model from 1 to 10 AU, J. Geophys. Res., 113, A08107, doi:10.1029/2008JA013046.